Local Regulation of Arterial Tone: an Insight into Wall Dynamics Using Mathematical Models

Etienne BOILEAU [1,*], Dimitris PARTHIMOS [2], Perumal NITHIARASU [1]

Corresponding author: Tel.: +44 (0)1792 604176; Email: e.boileau@swansea.ac.uk
1 Swansea University, Computational Bioengineering and Rheology, Swansea SA2 8PP, UK
2 Cardiff University School of Medicine, Institute of Molecular and Experimental Medicine, Wales Heart Research Institute, Cardiff CF14 4XN, UK

Abstract We present herein a first attempt to integrate large and small scale phenomena within an image-based computational domain. The aim of the present study is to highlight some of the underlying mechanisms that govern cellular interaction in the vascular wall, using a nonlinear model of vasomotion. We show that macroscopic rhythmic activity and emergent phenomena can indeed reflect ion movements at the level of the individual cell.

Keywords: Vasomotion, Smooth Muscle, Ion Calcium, Complex Dynamical System, Endothelium, Mass Transport, Computational Model

1. Introduction

Healthy vessels are characterised by an ability to adapt to the conditions imposed by the local environment, and respond to changes in blood flow by dilating or contracting. The progressive impairment of this dilator function is known as endothelial dysfunction, and it has been shown to predict long-term development of arterial disease (Halcox et al., 2002; Halcox et al., 2009; Schachinger et al., 2000).

The formation of atheromatic plaque in stenosed vessels is also an important area of modelling investigation (El Khatib et al., 2007; Cilla et al., 2014). In addition to the effects of hæmodynamics and transport, in early atheroma, there exists complex interactions between the arterial wall components, which cause inflammatory signalling that leads to monocyte accumulation, foam cell degeneration and formation of atheromatous plaque. Such alterations can result in significant modification of the arterial geometry. Many such factors can be incorporated in mathematical models, to gain insights into the interplay between disease processes and arterial function. The role of mathematical and computational modelling in studying cardiovascular disease as an integrated systemic dysfunction is therefore very important.

We propose a first attempt in this direction. A mathematical description of the ion transport systems that participate in the regulation of vascular tone is presented below. Computational results are shown for a population of coupled smooth muscle cells on the surface of an image-based domain. Modelling strategies are also discussed, with a view to add additional components of the arterial wall, including flow-endothelium interactions.

1.1 Arterial Structure and Function

The arterial wall consists of three layers. The first layer, the intima, is made up of a single lining of endothelial cells (ECs), the endothelium, supported by an internal elastic lamina that separates the intima from the second layer, the media. The endothelium forms a selective permeable membrane, and is a key actor in mediating the interactions between the lumen or flow domain and the

smooth muscle (SM) layer. The media is composed of smooth muscle cells (SMCs), embedded in a matrix of elastin and collagen fibres. In arterioles, it consists largely of SM. Changes in their contractile tension cause the vessel to dilate or constrict, thereby regulating vessel diameter and blood flow through the microcirculation.

The vascular SM is responsible for spontaneous fluctuations in vessel diameter that are not caused by changes in heart rate or blood pressure, and are referred to as 'vasomotion'. Vasomotion is thought to contribute to the enhancement of lymphatic drainage and microcirculatory mass transport, thereby reflecting the critical role of resistance vessels in regulating interstitial tissue pressure and delivery of oxygen and nutrients (Griffith, 1996).

The Smooth Muscle. The excitation-contraction coupling, or electrochemical coupling, is primarily controlled by movements of ion calcium Ca^{2+} into and out of the cytoplasm. Cytosolic Ca^{2+} concentration ($[Ca^{2+}]_i$) is normally maintained at a basal level of $\sim$ 100nm by the plasma membrane Ca^{2+}-ATPase (PMCA), the Na^{+}-Ca^{2+} exchanger (NCX) and the sarco endoplasmic reticulum Ca^{2+}-ATPase (SERCA). Vasoconstricting stimuli initiate SM contraction by increasing the $[Ca^{2+}]_i$, to reach the μm range. The rise in $[Ca^{2+}]_i$ is primarily mediated by voltage-(VOCCs) and store-operated channels (SOCs). The intracellular oscillator is identified by the cyclic Ca^{2+} -induced Ca^{2+} release from ryanodine-sensitive stores (RyR CICR) of the sarco endoplasmic reticulum (SR/ER) (Parthimos et al., 1999; Parthimos et al., 2007).

Membrane potential is a distinct dynamic variable determined by the additive contribution of a large number of ionic transport mechanisms, such as ion channels (Cl^{-}, K^{+}), pumps, and exchangers. The system of ordinary differential equations describing the coupling between the store-mediated intracellular Ca^{2+} oscillator and membrane potential fluctuations, due to ionic transport mechanisms across the cellular membrane, is presented below. For a detailed description, see Parthimos et al. (1999), Parthimos et al. (2007).

The Role of the Endothelium. Although smooth muscles are responsible for vascular tone and contractile phenomena, the endothelium act as an active interface between the lumen and the inner layers of the blood vessel wall. Electrical and chemical signalling between endothelial and SM cells thus contribute to arterial function in various ways. The role of the endothelium in vasomotion nevertheless remains unclear. Some studies reported rhythmic contractions in the absence of an intact endothelium, whereas others claimed that its presence is needed for synchronization (Peng et al., 2001; Sell et al., 2002; Okazaki et al., 2003).

Although the results presented below do not include any coupling between endothelial and SM cells, future work will address this point, in addition to considering the effects of mass transport on mobilization of endothelial $[Ca^{2+}]_i$. The release of the nucleotide adenosine-5' triphosphate (ATP) by endothelial cells, via wall shear stress (WSS)-dependent mechanisms, is thought to play a key role in endothelium-mediated vasodilation. Its influence on regional blood flow is also seen through the effects of its end-products, such as adenosine diphosphate (ADP). Flow regulation of ATP- and ADP-Ca^{2+} coupling in the concentration boundary-layer depends on several factors. Small changes in the model parameters, such as the rate constants for the degradation and/or production of ATP significantly influence the pattern of catalytic reactions at the endothelium (Boileau et al., 2013). As we have shown earlier, and as illustrated in Fig. 1, even though the bulk concentration of secreted agonists is low and mostly unaffected by the flow, variations exist at the endothelium, which are nevertheless difficult to quantify numerically. We hypothesize that signal transduction pathways could be altered by

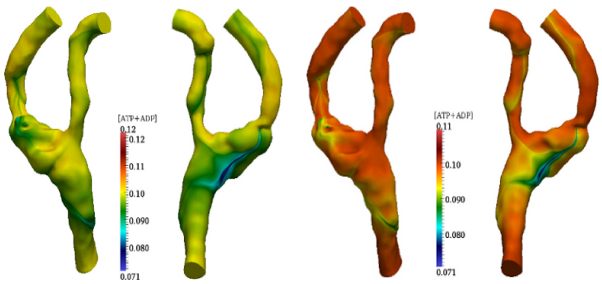

Figure 1: At two instants during diastole and systole. Intravascular concentration of nucleotides remains mostly insensitive to the reactions occurring at the endothelium. Signalling pathways may however be affected by the concentration boundary layer.

mass transport phenomena and reaction kinetics occuring at the vessel wall.

2. Model Formulation

Let $x = [Ca^{2+}]_i$ represent the cytosolic free Ca^{2+} concentration, $y=[Ca^{2+}]_{SR}$ the Ca^{2+} concentration in the sarcoplasmic reticulum and z the cell membrane potential, then the system of ordinary differential equations characterising vasomotion is the following:

where the electric reversal potentials with respect to Ca^{2+} and Na^{+} are determined from the Nernst equation. All values of the coefficients are found in Table 1. A complete description of the mathematical model can be found in Parthimos et al. (1999) and Parthimos et al. (2007). The subscript r refers to RyR-mediated CICR, as opposed to $InsP_3$ -induced Ca^{2+} release (not included in the present formulation).

3. Results of coupling SMCs-SMCs

The nature of coupling between adjacent cells remains difficult to ascertain. In the current formulation we explore the consequences of either Ca^{2+} or electrical coupling, by assuming a simple gradient driven flux between neighbouring cells coupled via gap junctions. The actual geometry of each SMC is not modelled explicitly. The mean cell surface area of is $\sim 143\mu m^2$.

All cells are dynamically identical except for the A parameter, which reflects influx of Ca^{2+} via non-specific cationic channels (NSCCs), and is randomly distributed around its mean value given in Table 1.

$$\frac{dx}{dt} = A - B\frac{x^n}{x^n + x_b^n} + C_r\frac{x^{p_r}}{x^{p_r} + x_r^{p_r}}\frac{y^{m_r}}{y^{m_r} + y_r^{m_r}} - Dx^k\left(1 + \frac{z - z_d}{R_d}\right) - E_{Ca}\frac{z - z_{Ca1}}{1 + e^{-(z - z_{Ca2})/R_{Ca}}} + E_{NCx}\frac{x}{x + x_{NCx}}(z - z_{NCx}) + Ly \quad (1a)$$

$$\frac{dy}{dt} = B\frac{x^n}{x^n + x_b^n} - C_r\frac{x^{p_r}}{x^{p_r} + x_r^{p_r}}\frac{y^{m_r}}{y^{m_r} + y_r^{m_r}} - Ly \quad (1b)$$

$$\frac{dz}{dt} = -\gamma\left(E_{Cl}\frac{x}{x + x_{Cl}}(z - z_{Cl}) + 2E_{Ca}\frac{z - z_{Ca1}}{1 + e^{-(z - z_{Ca2})/R_{Ca}}} + E_{NCx}\frac{x}{x + x_{NCx}}(z - z_{NCx}) + E_k(z - z_k)\frac{x}{x + \beta e^{-(z - z_{Ca3})/R_k}}\right) \quad (1c)$$

Hence the SMC population contains cells that are quiescent, in an under- or over-stimulated state, in terms of Ca^{2+} availability, and cells that are oscillating spontaneously. Within this range, the oscillatory regime is maintained at a physiological level.

Table 1. Coefficients

Parameter	Description	Value
A	Ca^{2+} influx via NSCC	$2.3\mu M s^{-1}$
L	SR leak rate constant	$0.025 s^{-1}$
γ	scaling factor (inverley related to cell capacitance)	$1V\,\mu M^{-1}$
VOCC influx		
E_{Ca}	whole cell conductance	$12\mu M\,V^{-1}\,s^{-1}$
z_{Ca1}	reversal potential	0.12 to 0.135V
z_{Ca2}	half point of activation sigmoid	−0.024V
R_{Ca}	max. slope of activation sigmoid	0.0085V
NCX		
$E_{Na/Ca}$	whole cell conductance	$43.8\mu M\,V^{-1}\,s^{-1}$
$z_{Na/Ca}$	reversal potential	−0.03 to −0.045V
$x_{Na/Ca}$	half point of Ca^{2+} activation	$0.5\mu M$
SR uptake		
B	rate constant	$400\mu M\,s^{-1}$
x_b	half point of ATPase activation sigmoid	$4.4\mu M$
n	Hill coefficient	2
RyR CICR		
C_r	rate constant	$1250\mu M\,s^{-1}$
y_r	half point of Ca^{2+} efflux sigmoid	$8.9\mu M$
x_r	half point of CICR activation sigmoid	$0.9\mu M$
m_r	Hill coefficient	2
p_r	Hill coefficient	4
Ca^{2+} extrusion by ATPase pump		
D	rate constant	$6.25\mu M\,s^{-1}$
z_d	intercept of voltage dependence	−0.1V
R_d	slope of voltage dependence	0.25V
k	exponent for $[Ca^{2+}]_i$ dependence	2
Cl^- channels		
E_{Cl}	whole cell conductance	$65\mu M\,V^{-1}\,s^{-1}$
z_{Cl}	reversal potential	−0.025V
x_{Cl}	Ca^{2+} sensitivity	$0\mu M$
k	exponent for $[Ca^{2+}]_i$ dependence	2
K^+ efflux		
E_K	whole cell conductance	$43\mu M\,V^{-1}\,s^{-1}$
z_K	reversal potential	−0.095V
z_{Ca3}	half point of K_{Ca} channel activation sigmoid	−0.027V
R_K	max. slope of K_{Ca} channel activation sigmoid	0.012V
β	Ca^{2+} sensitivity of K_{Ca} channel activation sigmoid	$0\mu M$

Weakly coupled cells are dominated by local dynamics and chaotic patterns. For stronger Ca^{2+} coupling, discrete pacemaker nodes become prominent, and these are eventually dominated by one or two nodes, resulting in clear wave fronts, as illustrated in Fig. 2.

This behaviour coincides with the synchronization of intracellular Ca^{2+} oscillations, showing that macroscopic rhythmic activity can indeed reflect ion movements at the level of the individual cell.

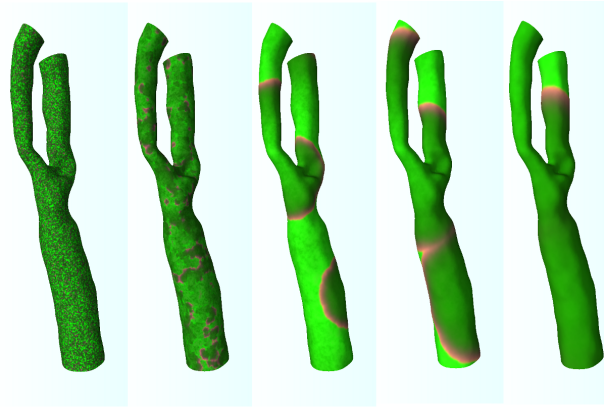

Figure 2: Computational modelling results illustrating the emergence of propagating wavefronts. A gradual transition of uncorrelated oscillatory activity into coherent patterns is observed under conditions of increased intercellular Ca^{2+} coupling from left to right. Colours are coded as: red=cytosolic free $[Ca^{2+}]_i$, green=$[Ca^{2+}]_{SR}$, blue=membrane potential. A magenta colour is seen where red and blue strengths are equal, and therefore indicative of membrane depolarization and high Ca^{2+}influx.

The interplay between extracellular Ca^{2+} influx via NSCCs and VOCCs was also investigated, although limited degree of synchronization was observed under conditions of purely electrical coupling. Simulations showed how low or high influx through either channel leads to the dominance of Ca^{2+} and/or electrical coupling, and to the loss of oscillatory activity.

The theoretical consequences of local neighbour interactions through electrical and/or chemical coupling have only been briefly presented, and will be further compared. Additional manifestations of blood-wall and arterial dynamics coupling will be investigated, and potential mechanisms underlying flow-endothelium interactions will be discussed.

References

Boileau E., Bevan RLT., Sazonov I., Nithiarasu P. (2013) Flow-induced ATP release in patient-specific arterial geometries: a comparative study of computational models. Intl. J. Numer. Method Biomed. Eng. 29, 1038–1056

El Khatib N., Genieys V., Volpert V. (2007) Atherosclerosis initiation modeled as an inflammatory process. Math. Model. Nat. Phenom. 2, 126-141.

Cilla M., Pena E., Martinez MA. (2014) Mathematical modelling of atheroma plaque formation and development in coronary arteries. J. R. Soc. Interface. 11, 20130866.

Griffith TM. (1996) Temporal chaos in the microcirculation. Cardiovasc. Res. 31, 342- 358.

Halcox, JPJ., Donald, AE., Ellins, E., et al. (2009) Endothelial function predicts progression of carotid intima-media thickness. Circ. 119, 1005-1012.

Halcox, JPJ., Schenke, WH., Zalos, G., et al. (2002) Prognostic value of coronary vascular endothelial dysfunction. Circ. 106, 653-658.

Okazaki K., Seki S., Kanaya J., et al. (2003) Role for the endothelium-derived hyperpolarizing factor in phenylephrine-induced oscillatory vasomotion in rat small mesenteric artery. Anesthesiology. 98, 1164-1171.

Parthimos, D., Edwards. DH., Griffith, TM. (1999) Minimal model of arterial chaos generated by coupled intracellular and membrane Ca2+ oscillators. Am. J. Physiol. 277, H1119–H1144.

Parthimos, D., Haddock, RE., Hill, CE., Griffith, TM. (2007) Dynamics of a three-variable nonlinear model of vasomotion: comparison of theory and experiments. Biophys. J. 93, 1534–1556.

Peng H., Matchkov A., Ivarsen A., et al. (2001) Hypothesis for the initiation of vasomotion. Circ. Res. 88, 810-815.

Schachinger, V., Britten, MB., Zeiher, AM. (2000) Prognostic impact of coronary vasodilator dysfunction on adverse long-term outcome of coronary heart disease. Circ. 101, 1899-1906.

Sell M., Boldt W., Markwardt F. (2002) Desynchronising effect of the endothelium on intracellular Ca2+ concentration dynamics in vascular smooth muscle cells of rat mesenteric arteries. Cell Calcium. 32, 105-120.